Cross-link density influence on the relaxations in glass- and gel-forming polyurethanes by neutron and Brillouin scattering

Y. Scheyer, C. Levelut, and J. Pelous
Laboratoire des Verres, Université Montpellier II, place E. Bataillon, cc 69, F-34095 Montpellier, France

D. Durand
Laboratoire de Physicochimie des Polymères, Université du Maine, F-72017 Le Mans, France

(Received 28 October 1997)

An experimental investigation of the relaxational processes related to the glass transition is presented in a family of polymers where the cross-link density as well as the length between cross links can be varied. We used inelastic light and neutron scattering to determine the relaxation times in the 10^{-8}–10^{-12} s range. The relaxation time determined from neutron scattering exhibits a Q^{-n} dependence, with $n \simeq 4$, and is more sensitive to variations of the cross-link density than Brillouin scattering is. However, the relaxation times measured by both techniques split from the structural relaxation determined at lower frequencies; they have a nearly Arrhenius behavior with approximately the same activation energy. The two high-frequency techniques probe the same secondary relaxation process. The dependence on the microscopical parameters of this process suggests that the corresponding relaxing entity can be identified as a small portion of the arms of the triol. [S0163-1829(98)07217-8]

I. INTRODUCTION

The freezing of a liquid into the glassy state constitutes one of the major poorly understood phenomena in condensed matter physics. The relaxational processes related to the glass transition have been extensively studied in fragile liquids (in Angell's classification[1]) and in polymers using many experimental techniques in a large frequency domain (from a few Hz to several GHz).[2,3] Whereas in the past most studies concerned the long or macroscopic time regime (above about 1 ps), many recent works involve inelastic neutron and light scattering techniques which are well suited for the study of short time dynamics. As a matter of fact, the dynamics in the picosecond range is specially interesting because of its implications on the microscopic mechanisms.

In many glass-forming liquids, a secondary process, usually called Johari-Goldstein β relaxation,[4] has been observed above the glass transition, in addition to the primary relaxation (α) which follows the changes of the viscosity. The long time α or ''structural'' relaxation is generally considered as cooperative and the relaxation time τ is well described by the Vogel-Fulcher-Tamman-Hesse equation. The β process exhibits an Arrhenius behavior.

The mode coupling theory of Götze and Sjögren also predicts[5,6] a two-step relaxation scenario and the existence of a fast β process in the picosecond range. A splitting between the two relaxational processes occurs in the neighborhood of the liquid-glass transition. The β process corresponds to the minimum in the susceptibility spectrum between the α process and the microscopic motions and its characteristic time exhibits power law divergences when approaching the temperature of the decoupling on both sides. The α region of the mode coupling theory is identical with the conventional α relaxation. The relaxation function (i.e., the response function at $t>0$ of a small perturbation slowly applied at $t \leqslant 0$ and switched off at $t=0$) of the α process is described by a stretched exponential $\exp[-(t/\tau)^{\beta}]$.

An alternative description referred to as Ngai coupling model[7,8] also introduces two relaxational processes: a Debye-like α_{fast} process, characterized by one single relaxation time, and a ''heterogeneous'' α_{slow} process characterized by a stretched exponential $\exp[-(t/\tau)^{1-n}]$, where n is related to the cooperativity of the relaxational process. There is a change of regime from the short time Debye process to the long time stretched exponential α_{slow} regime at a microscopic time t_c, which is temperature insensitive.

Clear evidence for the existence of a fast relaxation process preceding the α relaxation process was found by neutron and light scattering as well as by molecular dynamics simulations in the mixed salt CKN,[9,10] in polymers[11,12] and in the van der Waals liquid orthoterphenyl.[13,14]

We present a study of the relaxational processes on polymers belonging to the family of polyurethanes. The aim of this work is to make progress in the identification of the microscopic origin of the relaxation processes related to the glass transition T_g. By changing parameters such as the molecular weight of the triol and the cross-link density, it is possible to change the local structure at the scale of a few angstrom. Hence, the study of the influence of such parameters can be useful in identifying the origin of the relaxation processes.

II. SAMPLES AND PREVIOUS STUDIES

The polyurethanes are obtained from the polycondensation of two constituents, a triol and a diisocyanate. The OH and NCO groups react to form a urethane bound –O–CO–NH–. The reaction of a trifunctional constituent with a difunctional one can lead to a tridimensional network. We studied series of samples where the proportion of the two constituents, i.e., the ratio $r=[\text{NCO}]/[\text{OH}]$ of the reacting

groups NCO and OH, is changed; this allows us to vary the cross-link density. Each series (i.e., samples synthesized from the same triol) undergoes a gelation transition as a function of the ratio r. We studied samples corresponding to an excess of alcohol groups ($r<1$). The reaction was carried out at 313 K under a catalyst until there was complete consumption of the NCO groups. $r=0$ corresponds to the pure triol and $r=1$ to a completely connected sample (the reaction is achieved). The length between cross links can also be modified by changing the molecular weight of the triol used for the synthesis. We studied samples prepared using two different triols with molecular weights $m=700$ g mol^{-1} and $m=6000$ g mol^{-1}. In the following, the samples synthesized from the low-molecular-weight triol ($m=700$ g mol^{-1}) will be referred to as ''low-molecular-weight polyurethanes'' or LMPU and that synthesized from the high-molecular-weight triol as ''high-molecular-weight polyurethanes'' or HMPU. The gelation occurs for $r_c=0.56$ for the LMPU and $r_c=0.75$ for the HMPU. The glass transition temperature T_g is r dependent for the LMPU ($215<T_g<256$ K for $0<r<1$) and nearly r independent for the HMPU ($211<T_g<215$ K).

The structural relaxation is well documented in the polyurethane samples under study.[15] It has been studied at lower frequencies for the fully gelled samples synthesized from low-molecular-weight triol ($r=1$, $m=700$ g mol^{-1}) using dynamic light scattering, ultrasonic measurements, and dynamical mechanical thermal analysis. It is well described by a Vogel-Fulcher-Tamman-Hesse law.[15] At higher frequencies, Brillouin and inelastic neutron scattering have been used to characterize the relaxational process in several polyurethanes samples corresponding to different cross-link density and synthesized from the lower-molecular-weight triol ($m=700$ g mol^{-1}).[16] In this paper, we will study the influence of the cross-link density, via the parameter r, in the series of samples synthesized from the high-molecular-weight triol. We will evidence that the parameters r and m have different implications on the dynamics at the microscopic scale. We will also make a qualitative comparison of the relaxation times obtained by Brillouin scattering to those obtained by inelastic neutron scattering for both series.

III. BRILLOUIN SCATTERING

Brillouin spectra were registered in five LMPU and four HMPU samples, covering in both cases the whole available range of cross-link density. The measurements were performed using a 2×3 pass Fabry-Pérot interferometer, following Sandercock's design.[17] The experimental conditions are presented elsewhere.[16,18] We measured the signal scattered with the same polarization as the incident light [or vertical-vertical (VV) polarization]. In those samples, the signal scattered with a polarization different from that of the incident light [vertical-horizontal (VH) polarization] and due to the coupling of reorientational motions with the acoustic phonons is very weak (Fig. 1). The temperature range of investigation was about 200–373 K. It was not possible to measure at higher temperature because it could induce a degradation of the samples. This temperature range extends over the $(0.8-1.45)T_g$ to $(0.95-1.8)T_g$ depending on the sample. An example of evolution with the temperature of Brillouin spectra in sample $r=0.4$ from the HMPU set is shown in Fig. 2. The Brillouin spectra in polyurethanes in this temperature range are broad and asymmetric. This behavior can be interpreted in terms of relaxational modes coupled to acoustical modes. The maximum coupling of acoustic phonon and relaxational process is achieved when the spectra are the largest and the most asymmetric. This condition is fulfilled for $T=329$ K in the example of Fig. 2, whereas it was not possible to reach a temperature high enough to complete the condition in the LMPU samples. As described elsewhere,[18] the spectra can then be fitted using a general linearized hydrodynamic equation, where a Cole-Davidson distribution function is used to account for the nonexponentiality of the relaxational process:

$$S(q,\omega)=\frac{I_0}{\omega}\,\mathrm{Im}\left[\left(\frac{M^*q^2}{\rho}-\omega^2\right)^{-1}\right], \tag{1}$$

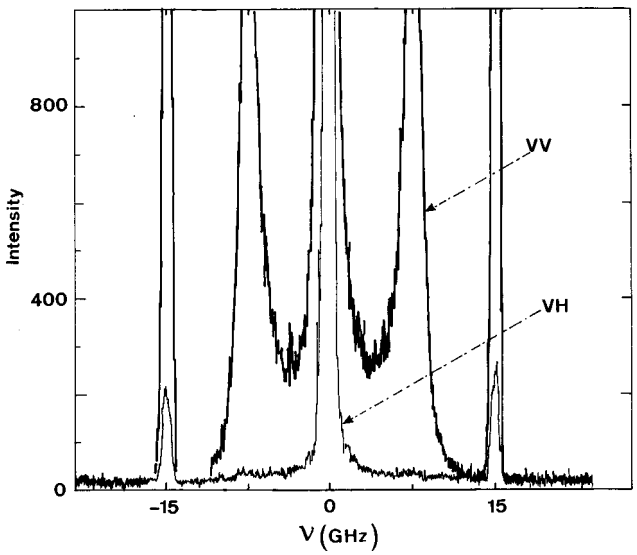

FIG. 1. Comparison of VV- and VH-polarized scattered light in a HMPU polyurethane sample corresponding to a ratio $r=0.4$ of reacting groups. The spectra are plotted as a function of the frequency $\nu=\omega/2\pi$.

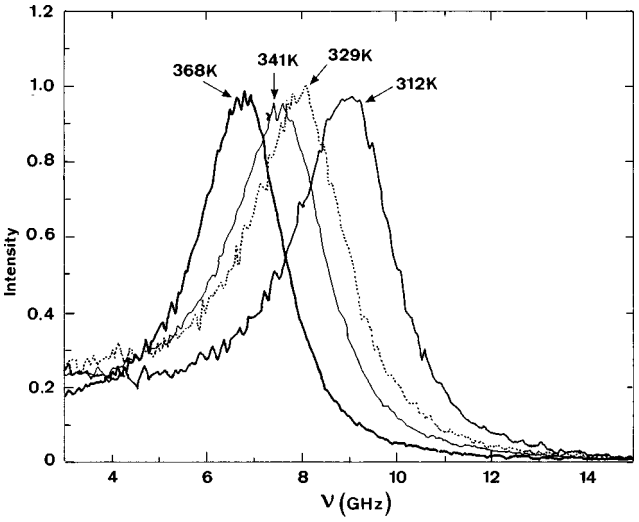

FIG. 2. Examples of Brillouin inelastic light scattering spectra taken in samples $r=0.4$ and $m=6000$ g mol^{-1} for several temperatures. The maximum coupling is achieved for $T=329$ K.

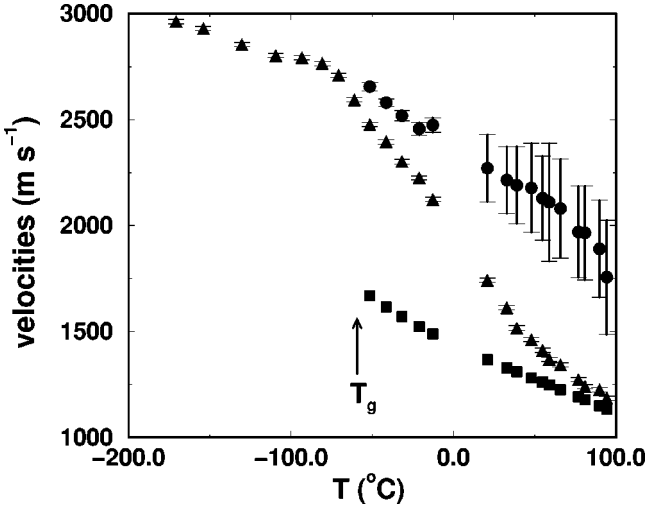

FIG. 3. Evolution with the temperature of the sound velocities V_B (▲), V_0 (■), and V_∞ (●) in the same sample as Fig. 2. V_B is determined from the position of the Brillouin peak, the high-frequency limit V_∞ is determined from the fit of the Brillouin spectrum, and V_0 is determined from ultrasonic measurements.

with

$$M^*/\rho = V_\infty^2 - \frac{V_\infty^2 - V_0^2}{(1+i\omega\tau)^{\beta_{CD}}}, \tag{2}$$

where M^* is the complex elastic modulus, and V_0 and V_∞ are the low- and high-frequency limits of the sound velocity. ρ is the density of the sample and τ is the characteristic time of the relaxational process which coupled to the acoustic phonon. This method was used only for temperatures above $T_g - 10$ K, where the coupling of the relaxational process with the acoustic phonon is strong enough to allow this kind of analysis.

The result of the fitting procedure yields the high-frequency limit of the sound velocity V_∞, which can be compared to the position of the Brillouin peak V_B. The low-frequency limit of the sound velocity V_0 was determined from ultrasonics measurements[19] and was fixed for the analysis of Brillouin data. The sound velocity V_B varies from a V_0 regime at high temperature, corresponding to a regime where the characteristic time of relaxation τ is such that $\omega\tau \ll 1$, to a V_∞ regime at low temperature, when $\omega\tau \gg 1$. Figure 3 presents an example of the temperature dependence of the velocities V_0, V_B, and V_∞ for the same sample as in Fig. 2, illustrating this behavior. The influence of the connectivity on the sound velocity is represented in Fig. 4(a) where the sound velocity V_B has been plotted for several LMPU and HMPU corresponding to several cross-link densities. For all the samples, the sound velocity slightly decreases with increasing temperature, up to the glass transition temperature, and then strongly decreases. For the LMPU, at fixed temperature, the sound velocity increases about 15% when r increases from 0 to 1. The material becomes more elastic with increasing connectivity. The sound velocity in HMPU does not significantly vary with r. This effect is correlated to the behavior of the glass transition temperature which does not vary with the connectivity for this set of samples. Moreover, the velocity curves for all the samples of both sets can

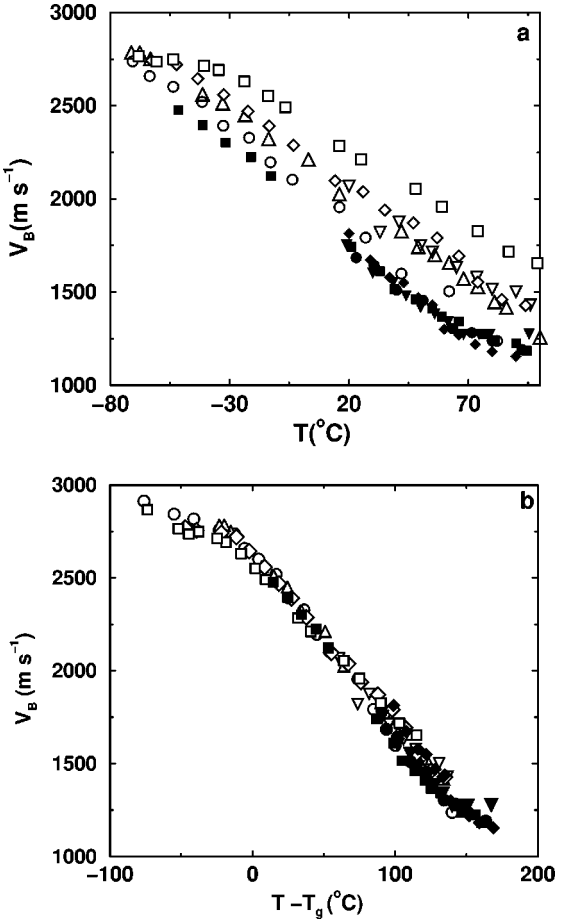

FIG. 4. (a) Influence of the cross-link density on the sound velocity V_B for both sets of samples, plotted as a function of temperature. (b) Rescaling of the sound velocities by $T - T_g$. The open symbols correspond to the LMPU set: $r=0$ (○), $r=0.3$ (△), $r=0.4$ (▽), $r=0.5$ (◇), and $r=1$ (□). The solid symbols correspond to the HMPU set: $r=0$ (●), $r=0.4$ (■), $r=0.76$ (▼), and $r=1$ (◆).

be rescaled when plotted as a function of $T - T_g$ [Fig. 4(b)]. So the elasticity at the hypersonic frequency scale reflects the same macroscopic behavior as the glass transition temperature.

On the other hand, the sound velocity is lower in the HMPU than in the LMPU. This can be understood by looking at the microstructure of the samples: in the HMPU series, the arms of the triol have more degrees of freedom than that of the LMPU, because they are longer; thus the material is softer and its elasticity is lower.

The exponent β_{CD} of the Cole-Davidson function does not depend significantly on the temperature, on the cross-link density, and on the molecular weight of the triol used for the synthesis. Its value is close to 0.2 for all the samples. As previously stated,[18] such a value can be converted to a stretched exponential exponent using several criteria which can be found in the literature.[20,21] The corresponding stretching exponent would be around 0.3–0.35 depending on the formula used for the conversion.

The mean times deduced $\langle\tau\rangle = \beta_{CD}$ from Brillouin data on sample $r=1$, $m=700$ g mol^{-1} above 310 K (for $1/T$ lower than 0.0032 K^{-1}) are in agreement with the extrapolation of the structural relaxation to high temperatures determined

from the low-frequency measurements.[15,16] However, at lower temperatures, the Brillouin-probed relaxational process splits from the α process and exhibits a nearly Arrhenius behavior in the $(1-1.6)T_g$ range and strongly diverges from the α process determined at lower frequency.[15,18] Such behavior has already been observed in many other studies carried out by Brillouin scattering[22–25] in glass-forming liquids. The authors of Ref. 25 attributed the relaxation probed by Brillouin scattering in polybutadiene to a strong coupling of the acoustical phonon to the α-bound torsional dynamics. In the particular case of $Ca_{0.4}K_{0.6}(NO_3)_{1.4}$, Cummins *et al.* interpreted the Brillouin-probed process as an α relaxation disturbed by the β process of the mode coupling theory. The authors showed that the discrepancy between the α relaxation and the Brillouin-probed process was an artifact of data analysis due to the neglect of the β process.[26] However, none of those explanations could be extended to all the materials in which such a discrepancy has been observed, and the nature of the relaxation probed by Brillouin is not elucidated.

Figure 5(a) shows the influence of the cross-link density for LMPU on the mean relaxation time: τ measured by light scattering increases with r. An approximately linear behavior is found[18] in the 270–370 K temperature range, which allows us to determine an apparent activation energy slightly increasing with r (E_a=30–38 kJ mol^{-1}). The values of the activation energy are reported in Table I. In a rescaled Arrhenius plot ($\log\langle\tau\rangle$ versus T_g/T), the relaxation times for all the samples synthesized from the low-molecular-weight triol are nearly superimposed in the $(1.1-1.5)T_g$ range [Fig. 5(b)]. The effect of the cross-link density can be fully described by taking into account the changes of T_g.[18] For the samples synthesized from the high-molecular-weight sample, the curves presenting the relaxation time as a function of the temperature in an Arrhenius plot for several cross-link densities are nearly indistinguishable: $\langle\tau\rangle$ seems to be r independent for the HMPU [see Fig. 5(a)]. Because the glass transition temperature also does not depend on the cross-link density, characterized by the ratio r, such behavior is in agreement with the fact that the variation of relaxation times is fully accounted for by changes in the glass transition temperature [Fig. 5(c)].

Moreover, the relaxation times for the HMPU are about 10 times lower than that of the low-molecular-weight samples (if one compares the fully connected polyurethanes). As for the variations of sound velocity, this effect can be related to the fact that the ''arms'' of the triol have more degrees of freedom in this series of samples, so that they can move faster. Moreover, because they are the most ''flexible'' part of the polyurethane molecule (compared to the ''rigid'' diisocyanate), they dominate the fast dynamics in the picosecond time range.

The ratio E_a/T_g, also reported in Table I, is slightly higher for the samples made of the triol of m=6000 g mol^{-1} than for the LMPU. This can be related to different ''space filling'' for two series. Indeed, in the LMPU the packing is only ruled by the connectivity and can be completely described by a percolation model. In contrast, in the high-molecular-weight triol, the arms are long enough to undergo entanglements, and this effect has to be taken into account in addition to the effect of connectivity.

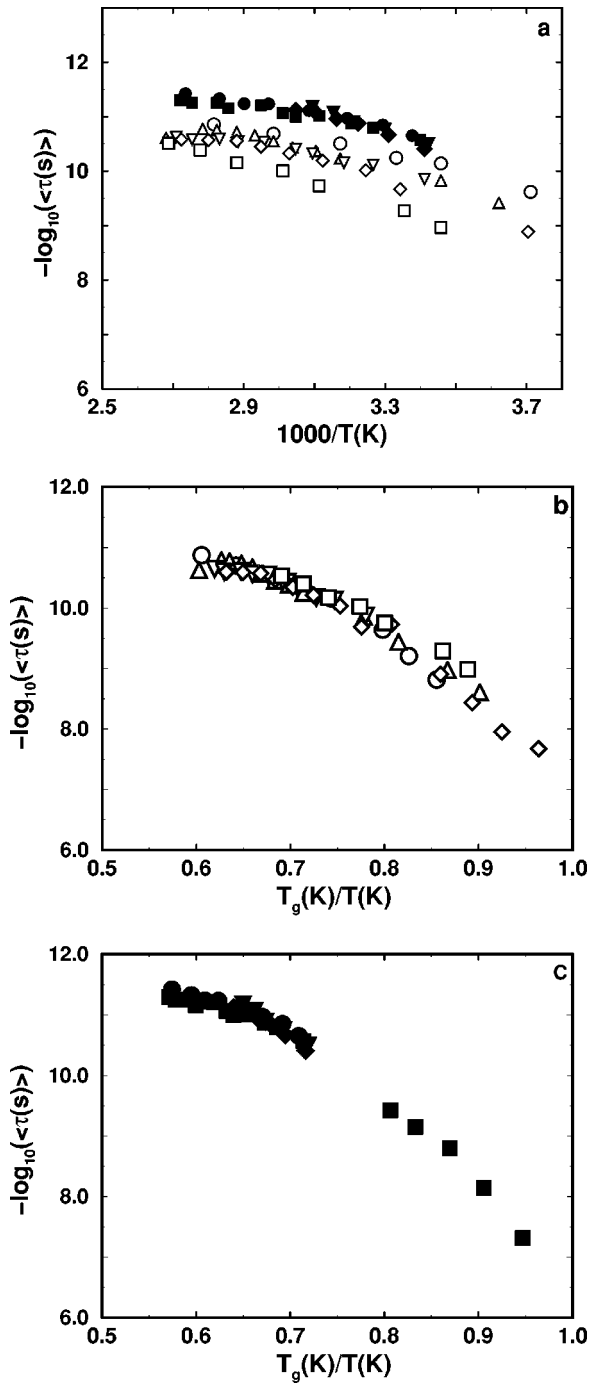

FIG. 5. (a) Arrhenius plot for five LMPU (open symbols) and four HMPU (solid symbols) samples. (b) Rescaled Arrhenius plot for LMPU. (c) Rescaled Arrhenius plot for HMPU. LMPU: r=0 (○), r=0.3 (△), r=0.4 (▽), r=0.5 (◇), and r=1 (□). HMPU: r=0 (●), r=0.4 (■), r=0.76 (▼), and r=1 (◆).

IV. INELASTIC NEUTRON SCATTERING EXPERIMENTS AND ANALYSIS

Inelastic neutron scattering spectra were measured using the time of flight spectrometers MIBEMOL of LLB (Saclay, France) and IN5 of ILL (Grenoble, France). Because of low count rates, we choose relatively thick samples, the measured transmission ranged between 90% and 80% depending on the wavelength of the measurements. Due to the high hydrogen contents of the samples, the scattering is essen-

TABLE I. Activation energy determined by Brillouin scattering and ratio of activation energy to glass transition temperature for the two series of samples.

m (g mol^{-1})	r	T_g (K)	E_a (kJ mol^{-1})	E_a/T_g (kJ mol^{-1} K^{-1})
700	0	220	31	0.14
	1	256	38	0.14
6000	0	210	35	0.165

tially incoherent. Hollow cylindrical sample geometry was chosen in order to keep self-absorption as isotropic as possible. The time of flight measurements were performed with an incident wavelength equal to $\lambda=8.5$ or 5.8 Å on MIBEMOL and $\lambda=5$ Å on IN5. The spectra were recorded in 508 time of flight channels and in about 300 ^{3}He detectors corresponding to 63 angles for MIBEMOL (1000 detectors and 90 angles for IN5). For both experiments the data were grouped into about 10 detectors groups, spread over of 3°–6°. The experimental conditions are reported in Table II.

The conversion of the data into a dynamic structure factor $S(2\theta,\omega)$ and the subtraction of container scattering were straightforward. The spectra were normalized to a vanadium standard. The spectra are then corrected from the Debye-Waller factor (determined from backscattering measurement on the IN10 spectrometer using the procedure defined in Ref. 27) and from the Bose factor. The function $S(2\theta,\omega)$ is unphysical because a constant detector angle 2θ does not correspond to a constant scattering vector Q: Q is given by the conservation law of momentum transfer:

$$Q=\left\{\frac{2m}{\hbar^2}[2E_i-\hbar\omega-2\cos 2\theta\sqrt{E_i(E_i-\hbar\omega)}]\right\}^{1/2}, \quad (3)$$

where $\hbar\omega$ is the energy lost by the incident neutron, m is the neutron mass, and $E_i=\hbar^2/2m\lambda^2$ is the incident energy of the neutrons of wavelength λ.

Figure 6 shows an example of Bose-scaled dynamic structure factor $S(Q,\omega)$ interpolated at constant Q value ($Q=1.2$ Å^{-1}) for several temperatures across the glass transition temperature measured in the completely connected HMPU sample ($r=1$, $m=6000$ g mol^{-1}), in a double-logarithm scale, to evidence the low-frequency part. The spectra are normalized to their maxima. The dominating feature of the spectra at low temperatures is the ''boson'' peak around 2 meV. This contribution arises from vibrational modes. At higher temperatures, a quasielastic broadening, whose intensity increases faster than the Bose factor, sets in. This broadening is characteristic of a relaxational process.

TABLE II. Experimental conditions used for the experiments: incident wavelength λ of the neutrons, energy resolution δE, and range of elastic wave vectors ΔQ and of scattering angles $\Delta\theta$.

Experiment	λ (Å)	δE (μeV)	ΔQ_{el} (Å^{-1})	$\Delta\theta$
MIBEMOL	8.5	35	0.3-1.13	11-128.7°
MIBEMOL	5.8	110	0.44-2	11-128.7°
IN5	5	100	0.24-2.26	23.5-141.8°

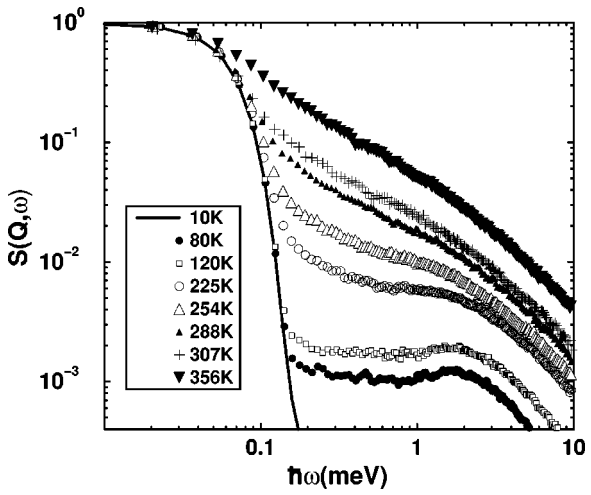

FIG. 6. Inelastic neutron scattering spectra measured by MIBEMOL (LLB, France) on the high-molecular-weight fully gelled sample for several temperatures, plotted in a log-log scale for a scattering vector $Q=1.2$ Å^{-1}. The spectra are normalized to their maxima. The solid line represents the 10 K spectrum, plotted to show the resolution.

As the quasielastic broadening due to the relaxation is of the order of the instrumental resolution width (a few tens of μeV), the analysis of the time of flight data recorded on MIBEMOL is performed using Fourier deconvolution of the measured spectra and fitting procedure in the time domain. The time correlation function $S(Q,t)$ is calculated from the Fourier transform of the data after interpolation to constant Q values. The accessible Q values are given by Eq. (3). Moreover, the available energy range depends on the Q value. The intermediate scattering function $S(Q,t)$ being calculated from the Fourier transform of $S(Q,\omega)$ can be evaluated only if the frequency spectrum includes the elastic channel $\omega=0$. This imposes severe restrictions upon the accessible energy and momentum transfers. For MIBEMOL experimental conditions, this condition leads to a maximum energy range $\hbar\omega\leqslant 6$ meV and $0.9\leqslant Q\leqslant 1.3$ Å^{-1} when λ is set to 8.5 Å and $\hbar\omega\leqslant 15$ meV and $0.9\leqslant Q\leqslant 1.9$ Å^{-1} when $\lambda=5.8$ Å. For IN5 experimental conditions, Q is in the 0.9–2.1 Å^{-1} range with $\hbar\omega\leqslant 15$ meV. The spectra are then symmetrized using detailed balance conditions to avoid truncature effects at zero frequency. The Fourier transform is calculated using a discrete Fourier transform algorithm, taking into account the limitation of time range required by Nyquist's theorem.[28] The Fourier transform of the experimental spectrum is divided by the Fourier transform of a low-temperature spectrum (10 K) in order to deconvolute from the resolution function. It has been previously shown[16] that, in our samples, a deconvolution from the vibrations following a procedure described in Ref. 12 yields very small differences between the deconvoluted Fourier transform obtained by both methods. The two methods differ only for the highest Q values (above $Q=1.6$ Å^{-1}) and the shortest times (below 4×10^{-13} s). In the conditions where the differences occur the result of the method of Ref. 12 gives very slightly higher τ values. However, this procedure neglects the temperature dependence of the vibrational contributions (softening of the boson peak with increasing temperature), and thus cannot produce quantitative correct values. Because in the

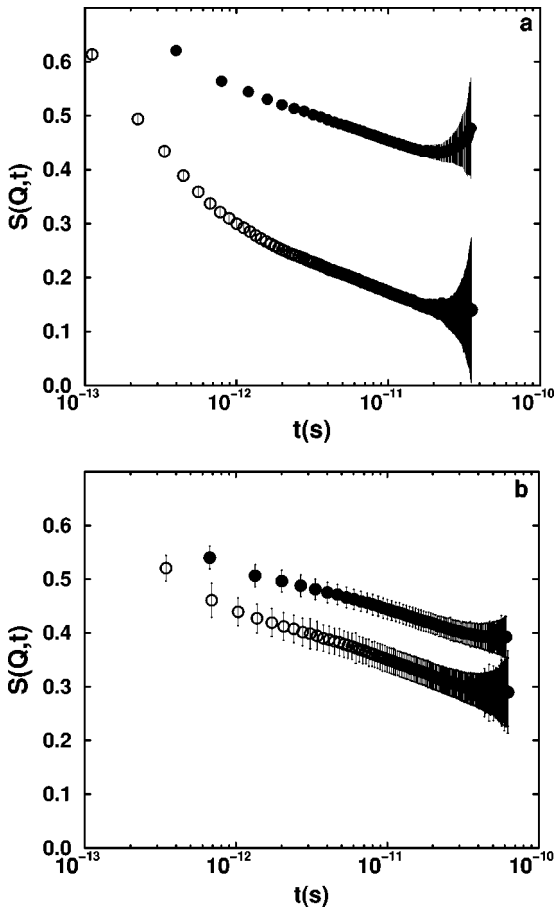

FIG. 7. Example of Fourier transform of time of flight data on MIBEMOL as a function of temperature, showing the error bars and the time domain of the Fourier transform. (a) $\lambda = 5$ Å for sample $r = 1$ in the LMPU set at 350 K, at $Q = 0.9$ Å^{-1} (●) and $Q = 2.1$ Å^{-1} (○). (b) $\lambda = 8.5$ Å, for the LMPU corresponding to $r = 0.6$ at 353 K at $Q = 0.9$ Å^{-1} (●) and $Q = 1.3$ Å^{-1} (○).

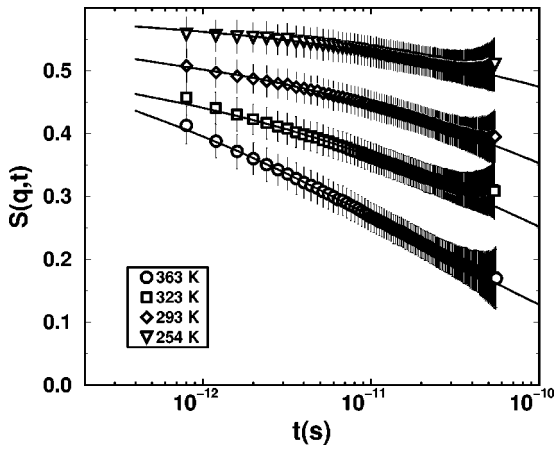

FIG. 8. Example of fits of the Fourier transform by a stretched exponential with exponent β fixed to 0.28. The Fourier transforms are calculated from time of flight data registered on MIBEMOL with $\lambda = 8.5$ Å and interpolated at $Q = 1.2$ Å^{-1} on sample $r = 0.6$, prepared from the triol of molecular weight $m = 700$ g mol^{-1}. The fits are shown for several temperatures above the glass transition temperature: 254 K (▽), 293 K (◇), 323 K (□), and 363 K (○).

frequency space the accessible energy range depends on the scattering vector value, in the time-space the minimum time value also depends on Q. Examples of the scattering law $S(q,t)$ is shown in Fig. 7 for one measurement carried out with $\lambda = 5$ Å [Fig. 7(a)] and one with $\lambda = 5$ Å [Fig. 7(b)], for the two extreme Q values. On the long time side, $S(q,t)$ has to be cut off above 5×10^{-11} s for $\lambda = 8.5$ Å and above 2×10^{-11} s for $\lambda = 5$ Å due to high errors bars at long times (see Fig. 7). Finally, the range in which the Fourier transform can be calculated is reported in Table III.

In our polyurethane experiments, the Fourier transform of the time of flight data does not demonstrate a two-step behavior, with a Debye process in the 10^{-13} ps range, as previously reported in other samples[29] and predicted by the Ngai coupling model. The scattering law in the full time range and at every Q value can be well fitted to a stretched exponential law (also called the Kohlrausch or William-Watt function) $S(Q,t) = S(Q,t=0)\exp[-(t/\tau)^{\beta_{KWW}}]$ in the 250–373 K temperature range. The mean relaxation time is calculated from the parameters of the distribution function using the relation $\langle\tau\rangle = \tau\Gamma(1/\beta_{KWW})$ where Γ denotes the gamma function. Since the dynamic window of individual spectra is restricted to less than two decades (about one and a half for $\lambda = 8.5$ Å), three-parameter fitting procedures yield huge error bars and inconsistent parameters. We assumed a time-superposition temperature i.e., we used a temperature-independent parameter β_{KWW}. The exponent β_{KWW} of the stretched exponential has been determined by performing systematic tests with fixed β_{KWW} values. The best simultaneous fits of all the spectra related to one given sample in the whole temperature range are obtained with a β_{KWW} exponent equal to 0.28 ± 0.02. This value is rather close to that of the stretched exponential exponent obtained from the conversion of the Cole-Davidson exponent deduced from the analysis of Brillouin data in polyurethanes. However, the quality of a single temperature fit is not very sensitive to the value of β_{KWW}, at least for the highest-temperature spectra. Rather good fits can be achieved within a certain range of β_{KWW}. Examples of fits at several temperature values for data measured with $\lambda = 8.5$ Å^{-1} for sample $r = 0.6$ of the LMPU set at $Q = 1.2$ Å^{-1} are shown in Fig. 8 for several temperatures above the glass transition temperature. In Fig. 9 is plotted the logarithm of the relaxation time for sample $r = 1$, $m = 700$ g mol^{-1} at several temperatures in the 238–363 K range as a function of the momentum transfer Q in a linear-logarithmic scale. The results include data obtained using two distinct

TABLE III. Available-time range for the Fourier transform. $\Delta t(Q_{\min})$ and $\Delta t(Q_{\max})$ indicate the time ranges accessible for the minimum and maximum scattering vector ($Q_{\min}$ and $Q_{\max}$), respectively.

λ (Å)	$Q_{\min}$ (Å^{-1})	$\Delta t(Q_{\min})$ (s)	$Q_{\max}$ (Å^{-1})	$\Delta t(Q_{\max})$ (s)
5 Å	0.9	5×10^{-13}–2×10^{-11}	2.1	10^{-13}–2×10^{-11}
8.5 Å	0.9	7×10^{-13}–5×10^{-11}	1.3	3×10^{-13}–5×10^{-11}

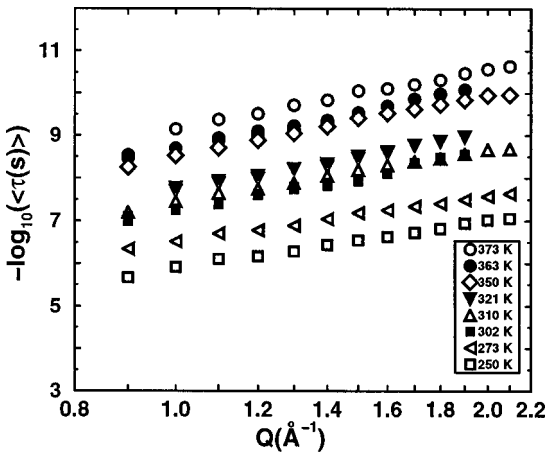

FIG. 9. Evolution of the mean relaxation time for a LMPU sample corresponding to $r=1$ as a function of the scattering vector Q. The measurements were carried out on IN5 with $\lambda=5$ Å (open symbols) and MIBEMOL $\lambda=5.8$ Å (solid symbols) in a wide temperature range.

experiments (IN5 with $\lambda=5$ Å and MIBEMOL with $\lambda=5.8$ Å). They are presented for Q ranging from 0.9 $Å^{-1}$ to 2.1 $Å^{-1}$. The curves are reasonably linear with approximately the same slope: this means that the behavior of τ as a function of Q is almost independent of the temperature in the temperature range of the measurements and within the experimental uncertainty. The fact that the Q behavior of $\tau(Q,T)$ is almost independent of the temperature in the temperature range of the measurements implies that $\tau(Q,T)$ can be factorized into a temperature-dependent term $a(T)$ and a Q-dependent term $\tilde{\tau}(Q)$. As can be seen in Fig. 10(a), a master curve $\tilde{\tau}(Q)$ can be built by shifting the $\tilde{\tau}(Q)$ values in the logarithmic scale towards the reference value $\tau(Q,T_R)$ where T_R is a temperature reference in the range of measurements.

The coefficients $a(T)$ which allow us to achieve the master curve are shown in Fig. 10(b). This coefficient gives the temperature dependence of the relaxation time determined by neutron scattering. The Brillouin determination of the relaxation time and the α process determined from low-frequency determination are also plotted for comparison. This figure shows that the process which contributes to the inelastic neutron scattering has a temperature dependence very similar to that of the Brillouin process. Both processes deviate from the α process for low temperatures (corresponding to $1000/T>3.2$).

The obtained ''master curves'' are shown in Fig. 10(c) for several samples. This figure shows that the variation of τ with the scattering vector in the 0.9–1.9 $Å^{-1}$ range is similar for several samples corresponding to various cross-link densities and synthesized from the two triols. Linear regressions of $\log\tau$ versus $\log Q$ give slopes ranging from $n=4.0\pm0.5$ for the LMPU with $r=0.4$ to $n=4.7\pm0.5$ for the HMPU $r=0$. The values of exponents n are given in Table IV. To summarize, the wide set of data is consistent with a $\tau\propto Q^{-n}$ law with $n=4.3\pm0.8$. A similar behavior has already been found by previous inelastic neutron studies in the same frequency range in poly(vinyl methyl ether) and in poly(dimethyl siloxane).[29–31] Such Q behavior is sometimes attributed to structural relaxation.[32]

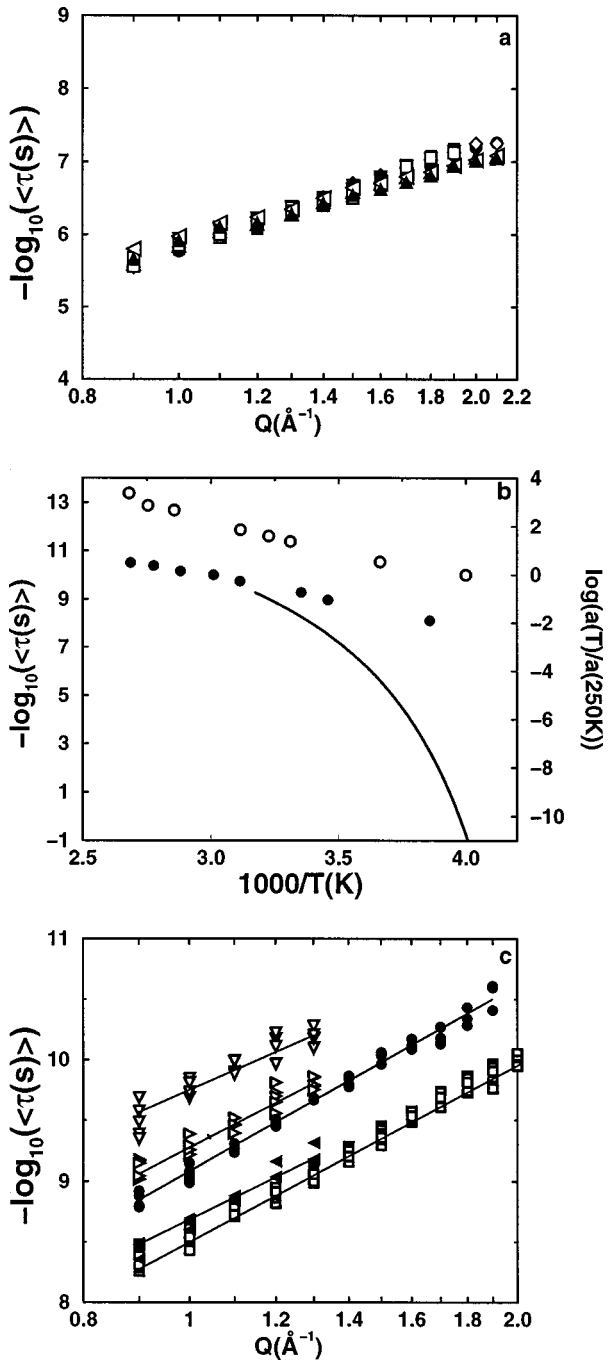

FIG. 10. (a) Master curve $\tilde{\tau}(Q)$ for sample $r=0.4$, prepared from the triol $m=700$ g mol^{-1} at a reference temperature 250 K. The solid line is a linear regression showing the Q^{-n} dependence of the relaxation times $\langle\tau\rangle$ with n close to 4. The values of $\tilde{\tau}(Q)$ are plotted for 250 K (▲), 273 K (▲), 302 K (□), 310 K (△), 321 K (▼), 350 K (◇), 363 K (■), and 373 K (●). (b) Temperature dependence of the coefficients used to build the master plot [$a(T)$, plotted as ○, vs $1000/T$]. Comparison with the logarithm of the relaxation times obtained from Brillouin scattering (●) and from the low-frequency techniques for the α process (solid line). (c) Similar master curve for several polyurethanes. The open symbols correspond to the LMPU set: $r=0.4$ (▽), $r=0.6$ (▷), and $r=1$ (□). The solid symbols correspond to the HMPU: $r=0$ (●) and $r=1$ (◆).

TABLE IV. Exponent n of the power law $\tau \propto Q^{-n}$ derived from the linear regression of the master curve $\tilde{\tau}(Q)$ vs Q for all the temperatures. n is reported for the six samples studied by time of flight, together with the range of temperature (indicated by the corresponding ratio T/T_g) where the linear regression has been performed.

m (g mol^{-1})	6000	6000	6000	700	700	700
r	0	0.8	1	0.4	0.6	1
T/T_g	1.4–1.7	1.4–1.7	1.4 –1.7	1–1.6	1–1.5	1–1.4
n	4.7±0.7	4.5±0.4	4.6±0.7	4.0±0.5	4.7±0.5	4.7±0.4

In the range of measurements, the temperature dependence is compatible with an Arrhenius behavior. Figure 11 shows the Arrhenius behavior for fully connected LMPU for several values of the momentum transfer Q between 0.9 and 2.1 Å^{-1}. The curves are nearly parallel; the activation energy does not significantly depend on the Q value. For this sample, a linear regression of the relaxation time for one given scattering vector is between 40 ± 2 kJ mol^{-1} and 49 ± 1 kJ mol^{-1} depending on the Q value. A linear regression of all the data points at the same time for the same sample gives a value $E_a = 45\pm5$ kJ mol^{-1}.

This behavior (activation energy independent of Q) is similar for all the samples. The activation energies obtained by linear regression over the relaxation times determined for all the Q values at the same time are given in Table V for several samples belonging to both series. The activation energies are around $E_a = 47\pm5$ kJ mol^{-1} and do not depend on either r or m, within the experimental accuracy.

The relaxation times measured for all the samples by inelastic time of flight neutron scattering with $Q = 1.2$ Å^{-1} are shown in an Arrhenius plot in Fig. 12. The relaxation time exhibits the same variations with the parameters r and m as does the time deduced from the inelastic light scattering data. The characteristic time for the relaxational process increases with increasing r for the LMPU samples and decreases with increasing m, of about one decade. Nevertheless, there is a difference between the two techniques: using neutron scattering, the relaxation time slightly depends on the cross-link density for the series of sample synthesized from the high-molecular-weight triol (the relaxation time for sample $r=1$ is about 3 times higher than for $r=0$). As a consequence, the relaxation times deduced from neutron scattering are not superimposed as plotted versus T_g/T for HMPU samples (Fig. 13). The superimposition is neither achieved for the samples synthesized from the low-molecular-weight triol: the amplitude of the effect on $\log\tau$ is higher than the variations of the glass transition temperature.

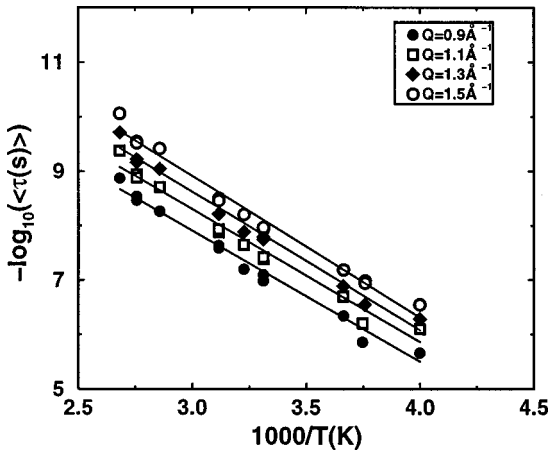

FIG. 11. Arrhenius plot $[-\log(\langle\tau\rangle)$ vs $1000/T]$ for the sample $r=1$ from the high-molecular-weight set. τ is determined from the fit with a stretched exponential of the Fourier transform of the time of flight data recorded with $\lambda = 5$ Å, for several scattering vector values ranging from 0.9 Å^{-1} to 2.1 Å^{-1}.

V. DISCUSSION

We have presented inelastic light (Brillouin) scattering and inelastic neutron (time of flight) scattering measurements in two series of polyurethane samples. In each series, the cross-link density is varied by changing the ratio r of two constituents: a triol and a diisocyanate. The two series differ by the molecular weight of the initial triol, which changes the length between cross links. Those two parameters change the microstructure and their influence on the relaxation time is tested.

A. Q dependence of neutron scattering data

Inelastic neutron scattering gives access, in addition to the ''classical'' temperature dependence, to the variations with another parameter: the scattering vector. The relaxation time decreases with increasing Q, following a Q^{-n} behavior, where n is close to 4. This behavior implies that the Gaussian approximation ($n \simeq 2$) does not hold for the polyurethane samples; this result is contradictory to what was found for several other polymers.[32] A Q^{-4} law was predicted by de Gennes for the incoherent scattering of a Rouse chain[33] but this model applies only for very small scattering vector (about 10^{-3} Å^{-1}).

Other authors mentioned that if the Gaussian approximation holds, then $S(Q,\omega) \propto \exp[-Q^2\langle u^2(T)\rangle]$ and $S(Q,\omega) \propto \exp(-At^{\beta_{KWW}}Q^{n\beta_{KWW}})$, where A is a constant, so that $n\beta_{KWW} \simeq 2$.[32] Then, the displacement of the scattering centers is independent of Q and governed by sublinear diffusion

TABLE V. Activation energy determined from the neutron time of flight measurements.

$m = 700$ g mol^{-1}	$r=0.4$	$E_a = 44.5\pm4$ kJ mol^{-1}
	$r=0.6$	$E_a = 47.5\pm1$ kJ mol^{-1}
	$r=1$	$E_a = 45\pm5$ kJ mol^{-1}
$m = 6000$ g mol^{-1}	r=0	$E_a = 51.5\pm2$ kJ mol^{-1}
	$r=0.8$	$E_a = 46\pm2$ kJ mol^{-1}
	$r=1$	$E_a = 51\pm2$ kJ mol^{-1}

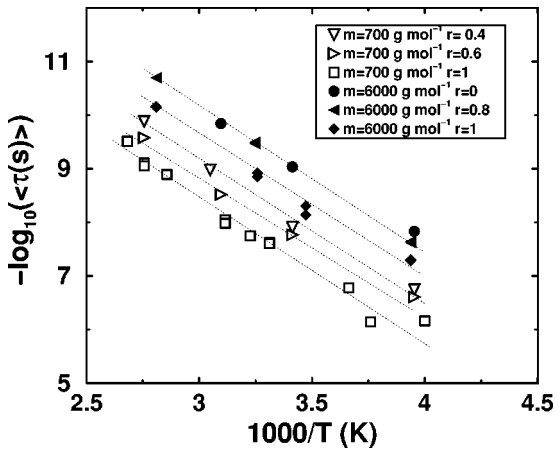

FIG. 12. Mean relaxation times for $Q=1.2$ Å^{-1} derived from inelastic neutron scattering presented in an Arrhenius plot for three LMPU and three LMPU samples. The dotted lines are guides for the eyes.

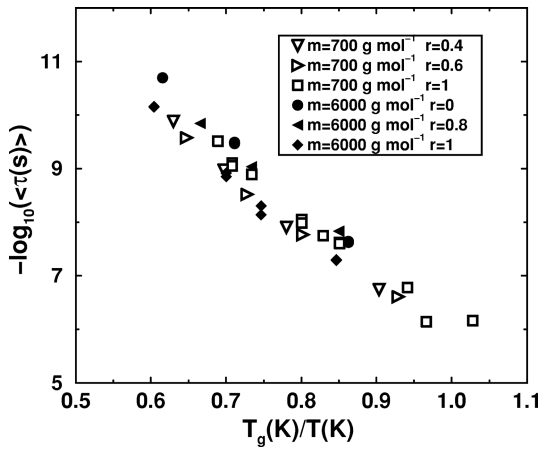

FIG. 13. Rescaled Arrhenius plot $\log(\langle\tau\rangle)$ vs T/T_g for the relaxation times deduced from the time of flight data for all the samples, plotted for $Q=1.2$ Å^{-1}.

$[\langle u^2(T)\rangle \propto t^{\beta_{KWW}}]$. Such behavior was observed in several polymeric glass-forming systems. In polyurethane samples, this relation is not fulfilled: we obtain $n\beta_{KWW}\simeq 1.3-1.6$, even if the exponent β_{KWW} is varied within the range of reasonable quality of fit. Hence, these samples deviate from the Gaussian behavior. Such a result was also found for polybutadiene and polyisopropylene.[34] Nevertheless, the calculated time dependence was similar for all the Q values investigated and the behavior found can be written as $f(t)=(6/Q^b)\ln[1/S(Q,t)]$ where $b<2$ is determined as the exponent for which the curves $(6/Q^b)\ln[1/S(Q,t)]$ are superimposed for every Q.[34] In polyurethanes, this analysis yields $b\simeq 0.7$ which confirms the non-Gaussian behavior. A β_{KWW} value can also be determined from the slope of the curves $(6/Q^b)\ln[1/S(Q,t)]$ in a log-log plot. This procedure yields $\beta_{KWW}\simeq 0.2$, slightly lower than the value determined from the best fits.

B. Comparison of Brillouin and inelastic neutron results

1. Wave-vector dependence

The Q dependence law of the relaxation time determined by time of flight is very strong. Hence, if this law would be extrapolated to the scattering vector of Brillouin scattering, assuming that both techniques probed the same process in a similar fashion, it would give a very long time scale for Brillouin scattering, different from the result we obtained. It is highly improbable that the observed Q dependence for neutron scattering can be extrapolated over three decades of Q. Moreover, the Q dependence is expected to be different for both techniques because, in the polyurethane samples, the inelastic neutron measurements are dominated by the incoherent scattering of the hydrogen atoms, whereas the Brillouin scattering is a coherent scattering. The Q dependence of coherent and incoherent scattering in the same Q range is expected to be very different because the coherent scattering vector dependence is modulated by the elastic structure factor. However, at the spatial scale of Brillouin scattering, there is no particular feature in the elastic structure factor. On the other hand, because of their coherent character for one and incoherent character for the other, the two techniques are not expected to reveal the same scattering behavior. Coherent scattering is expected to probe correlated motions, whereas incoherent neutron scattering is mostly sensitive to individual motions of hydrogen atoms. Nevertheless, in Brillouin scattering, the coupling with relaxational motions is indirect, so that we probe the correlated thermal motions which result in an acoustic phonon, but the relaxational motions coupled to the phonon are not necessarily correlated.

However, though the scattering vectors of the two techniques differ by three orders of magnitude and one is a coherent technique whereas the other one is incoherent, there are very strong analogies between the relaxations times probed by the two techniques.

2. Dependence on the microscopical parameters

First, the relaxation times determined by both techniques are in the same range. Second, they are both sensitive, in a similar manner, to changes of the connectivity (variations of r) and to changes of the length between cross links without changing the connectivity (variations of m). As already mentioned, the relaxation time increases when the cross-link density increases and decreases when the lengths between cross link increase; this behavior can be understood by assuming that the dynamics could be dominated by the movements of the ''arms'' of the triol. Increasing the ratio of the reacting groups and decreasing the molecular weight of the initial triol are two different ways to decrease the mean distance along the chains between cross links, i.e., the length of the chains of triol connected to each other by urethane bonds. The urethane bounds cannot contribute to the relaxation because the observed process is already present in pure triol with sensibly the same activation energy. Both effects (an increase of r and a decrease of m) cause an increase of the relaxation time. However, the two parameters have slightly different influences. The effect of m is of the same amplitude for the two techniques (whatever the scattering vector value is): about one decade for the fully connected samples, decreasing with decreasing r. In addition, this effect is not completely explained by the variations of the glass transition temperature. As a matter of fact, in Brillouin scattering, the

two sets of samples correspond to a different ratio E_a/T_g. By inelastic neutron scattering, the accuracy in the determination of the activation energy is not good enough to claim that the two series correspond to different ratios of activation energy to glass transition temperature, but the data corresponding to two samples, each synthesized from a different triol, are clearly not superimposed. The effect of r depends on the technique and is completely taken into account by the macroscopic effect of the glass transition temperature for the relaxation times determined using Brillouin scattering. However, the relaxation time probed by inelastic time of flight neutron scattering is more sensitive to the cross-link density than by Brillouin scattering. Several explanations can be suggested for a difference in behavior between the relaxational process probed by both techniques.

First of all, one possible difference comes from the different energy ranges investigated ($\hbar\omega$ is equal to a few meV for the time of flight whereas $\hbar\omega$ is about a few μeV for the Brillouin scattering).

Second, as already pointed out, the two techniques probe very different ranges of wave vector: Q is equal to a few Å^{-1} for the neutron scattering whereas $Q \simeq 1\times10^{-3}$ Å^{-1} for light scattering. Consequently, they are sensitive to the relaxation process at a very different spatial scale. Inelastic neutron scattering is a more local technique than Brillouin scattering; it is more sensitive to the microstructure and to the presence or the absence of cross-link points. At the larger scale probed by Brillouin scattering, much larger than the distance between cross links, the effect of cross links is likely to be smoothed by an effect of spatial averaging.

A third reason for the differences arises from the fact that the coupling of the relaxational process to light scattering occurs in an indirect fashion, via the coupling of the relaxation with an acoustic phonon which modifies the scattering of light by this acoustic phonon. In this case, the scattering vector Q corresponds to the scattering vector of the acoustic phonon and not to that of the relaxational excitation. Thus, this suggests that the acoustic phonon can couple to excitations of various scattering vectors and it can be sensitive to a broader distribution of relaxing entities. As pointed out in Sec. IV, the inelastic neutron spectra can also be analyzed with slightly larger values of β_{KWW}. This gives another argument in favor of a possibly larger time distribution observed by Brillouin scattering than that probed by inelastic neutron scattering.

3. Temperature dependence

The third analogy between the relaxation processes probed by the two techniques lies in their very similar temperature dependence. The relaxation processes probed by both techniques strongly deviate from the low-frequency determination of the α process. The coefficient $a(T)$ representing the temperature dependence of the relaxation time determined from time of flight measurements and the relaxation time measured from Brillouin scattering have very similar variations with the temperature. Both quantities exhibit a nearly Arrhenius behavior in the range of measurements. The activation energies deduced from the two techniques are of the same order of magnitude: about 35–50 kJ mol^{-1}. To figure out what kind of relaxing entity could correspond to such energy, we compared this value to the activation energy of the rotation of a CH_3 or a small lateral group (less than 15 kJ mol^{-1}); the conformational changes are usually characterized by activation energy below 10 or 20 kJ mol^{-1}.[25,35] Thus, the entity involved in the relaxational process responsible for the inelastic neutron scattering and which coupled to the acoustic phonon is of an intermediate size, involving something more difficult to move than a lateral group or a single C–C bond. We estimate that this entity includes at least three or four carbon atoms. The relaxational process studied in this paper is a semilocal one.

VI. CONCLUSION

In conclusion, the relaxation times determined using both techniques are of the same order of magnitude; their variations with either the microscopical parameters (the cross-link density and the length between cross links) or the physical ones (like the temperature) are very similar, and thus they are very likely to probe the same relaxational process. The differences between the times obtained from the two techniques (in the sensitivity to the cross-link density) arise from the techniques and the mechanism through which the relaxational process is probed. On the other hand, the process probed by inelastic light and neutron time of flight departs from the structural relaxation. Hence, the two techniques evidenced a secondary relaxation. Most studies carried out in polymers with time of flight experiments report a two-step regime with a Debye-like process below 10^{-12} s and the structural α relaxation process in the 10^{-12}–10^{-10} s range, i.e., in the main part of the time range available by the time of flight technique. The latter corresponds to a Q dependence corresponding to Q^{-n} with $n\beta_{KWW} \simeq 2$.[32,12,34] In poly(vinyl chloride), the Debye process was attributed to the β relaxation of the mode coupling theory and was found to be different from the β process measured by dielectric spectroscopy.[36] In some cases, a crossover between the α process and the β process was evidenced using mode coupling analysis.[37–39] However, in the polyurethanes, the intermediate scattering function does not exhibit a two-step behavior and the whole set of data could be fitted using only one memory function in the whole time, temperature, and scattering vector range.

To summarize, we evidenced a secondary relaxation in polyurethane by inelastic light scattering and inelastic neutron scattering. This result is in contrast with the results of previous measurements, with similar experimental conditions, in many other polymers.[32] Indeed, we probed a secondary (β) process instead of the α process evidenced in other polymers in this range of time and temperature. This process has an activation energy of about 35–50 kJ mol^{-1}, larger than the usual values of activation energy for secondary processes evidenced by other techniques. The relaxing entity contains about three or four carbon atoms and belongs to the arms of the triols.

ACKNOWLEDGMENTS

We are grateful for the facilities given by the ILL at Grenoble and the LLB at Saclay for neutron scattering measurements, as well as for the help of H. Casalta and R. Kahn for the measurements.

[1] C. A. Angell, J. Non-Cryst. Solids **131-133**, 378 (1991).
[2] E. Rössler and H. Sillescu, in *Glasses and Amorphous Materials*, Materials Science and Technology, Vol. 9, edited by J. Zarzycki (VCH, New York, 1991).
[3] E. Schlosser and A. Schönhals, Colloid Polym. Sci. **267**, 133 (1989).
[4] G. P. Johari and J. Goldstein, J. Chem. Phys. **53**, 2372 (1970).
[5] W. Götze and L. Sjögren, Rep. Prog. Phys. **55**, 241 (1922).
[6] W. Götze and L. Sjögren, Transp. Theory Stat. Phys. **24**, 801 (1994).
[7] K. L. Ngai, Comments Solid State Phys. **9**, 121 (1979).
[8] K. L. Ngai, C. Cramer, T. Saatkamp, and K. Funke, in *Non-Equilibrium Phenomena in Supercooled Fluids, Glasses and Amorphous Materials*, edited by M. Giordano, D. Leporini, and M. P. Tosi (World Scientific, Singapore, 1996).
[9] W. Knaak, F. Mezei, and B. Farago, Europhys. Lett. **7**, 527 (1988).
[10] G. Li, W. M. Du, X. K. Chen, H. Z. Cummins, and N. J. Tao, Phys. Rev. A **45**, 3867 (1992).
[11] D. Richter, B. Frick, and B. Farago, Phys. Rev. Lett. **61**, 2465 (1988).
[12] J. Colmenero, A. Arbe, and A. Alegría, Phys. Rev. Lett. **71**, 2603 (1993).
[13] W. Petry, E. Bartsch, F. Fujara, M. Kiebel, H. Sillescu, and B. Farago, Z. Phys. B **83**, 175 (1991).
[14] L. J. Lewis and G. Wahnström, Phys. Rev. E **50**, 3865 (1994).
[15] M. Tabellout, P.-Y. Baillif, H. Randrianatoandro, F. Litzinger, J. R. Emery, T. Nicolai, and D. Durand, Phys. Rev. B **51**, 12 295 (1995).
[16] C. Levelut, Y. Scheyer, J. Pelous, and F. Prochazka, J. Non-Cryst. Solids (to be published).
[17] J. R. Sandercock, J. Phys. E **9**, 566 (1976).
[18] C. Levelut, Y. Scheyer, M. Boissier, J. Pelous, D. Durand, and J. R. Emery, J. Phys.: Condens. Matter **8**, 941 (1996).
[19] J. R. Emery, D. Durand, M. Tabellout, and R. A. Pethrick, Polymer **28**, 1435 (1987); D. Durand (unpublished).
[20] C. P. Lindsey and G. D. Patterson, J. Chem. Phys. **73**, 3348 (1980).
[21] F. Alvarez, A. Alegría, and J. Colmenero, Phys. Rev. B **44**, 7306 (1991).
[22] D. Fioretto, L. Palmieri, G. Socino, and L. Verdini, J. Phys.: Condens. Matter **6**, 5295 (1994).
[23] G. Floudas, G. Fytas, and I. Alig, Polymer **32**, 2307 (1991).
[24] C. H. Wang, G. Fytas, and J. Zhang, J. Chem. Phys. **82**, 3405 (1985).
[25] A. Aouadi, M.-J. Lebon, C. Dreyfus, B. Strube, W. Steffen, A. Patkowski, and R. M. Pick, J. Phys.: Condens. Matter **9**, 3803 (1997).
[26] H. Z. Cummins, G. Li, W. Du, and M. Hernandez, J. Non-Cryst. Solids **172-174**, 26 (1994).
[27] B. Frick and D. Richter, Phys. Rev. B **47**, 14 795 (1993).
[28] W. H. Press, B. P. Plannery, S. A. Teukolsky, and W. T. Vetterling, *Numerical Recipes, the Art of Scientific Computing* (Cambridge University Press, Cambridge, England, 1986).
[29] J. Colmenero, A. Alegría, J. M. Alberdi, F. Alvarez, and B. Frick, Phys. Rev. B **44**, 7321 (1991).
[30] G. Floudas, J. S. Higgins, and G. Fytas, J. Chem. Phys. **96**, 7672 (1992).
[31] G. Allen, J. S. Higgins, A. Macounachie, and R. E. Ghosh, J. Chem. Soc. Faraday Trans. 2 **78**, 2117 (1982).
[32] J. Colmenero, A. Alegría, A. Arbe, and B. Frick, Physica B **182**, 369 (1992).
[33] P. G. De Gennes, Physics (Long Island City, N.Y.) **3**, 37 (1967).
[34] R. Zorn, A. Arbe, J. Colmenero, B. Frick, D. Richter, and U. Buchenau, Phys. Rev. E **52**, 781 (1995).
[35] J. P. Lowe, Prog. Phys. Org. Chem. **6**, 1 (1968).
[36] J. Colmenero, A. Arbe, and A. Alegría, Physica A **201**, 447 (1993).
[37] B. Frick, R. Zorn, D. Richter, and B. Farago, J. Non-Cryst. Solids **131-133**, 169 (1991).
[38] J. Wuttke, M. Kiebel, E. Bartsch, F. Fujara, W. Petry, and H. Sillescu, Z. Phys. B **91**, 357 (1993).
[39] B. Frick, D. Richter, R. Zorn, and L. J. Fetters, J. Non-Cryst. Solids **172-174**, 272 (1994).